



## Triterpenoids as inhibitors of erythrocytic and liver stages of *Plasmodium* infections

Cátia Ramalhete<sup>a</sup>, Filipa P. da Cruz<sup>b</sup>, Dinora Lopes<sup>c</sup>, Silva Mulhovo<sup>d</sup>, Virgílio E. Rosário<sup>c</sup>, Miguel Prudêncio<sup>b</sup>, Maria-José U. Ferreira<sup>a,\*</sup>

<sup>a</sup> iMed.UL, Faculdade de Farmácia, Universidade de Lisboa, Av. Prof. Gama Pinto, 1649-003 Lisboa, Portugal

<sup>b</sup> Instituto de Medicina Molecular, Faculdade de Medicina, Universidade de Lisboa, 1649-028 Lisboa, Portugal

<sup>c</sup> CMDT.LA, Instituto de Higiene e Medicina Tropical, UNL, R. da Junqueira 96, 1349-008 Lisbon, Portugal

<sup>d</sup> Escola Superior Técnica, Departamento de Ciências Agro-Pecuárias, Universidade Pedagógica, Campus de Lhanguene, Mozambique

### ARTICLE INFO

#### Article history:

Received 2 August 2011

Revised 7 October 2011

Accepted 14 October 2011

Available online 20 October 2011

#### Keywords:

Antimalarials

*Plasmodium*

Schizontocidal activity

Triterpenoids

Cucurbitacins

*Momordica balsamina*

### ABSTRACT

Bioassay-guided fractionation of the methanol extract of *Momordica balsamina* led to the isolation of two new cucurbitane-type triterpenoids, balsaminol F (**1**) and balsaminoside B (**2**), along with the known glycosylated cucurbitacins, cucurbita-5,24-diene-3 $\beta$ ,23(*R*)-diol-7-*O*- $\beta$ -*D*-glucopyranoside (**3**) and kuguaglycoside A (**4**). Compound **1** was acylated yielding two new triesters, triacetyl balsaminol F (**5**) and tribenzoyl balsaminol F (**6**). The structures were elucidated based on spectroscopic methods including 2D-NMR experiments (COSY, HMQC, HMBC and NOESY). Compounds **1–6**, were evaluated for their antimalarial activity against the erythrocytic stages of the *Plasmodium falciparum* chloroquine-sensitive strain 3D7 and the chloroquine-resistant clone Dd2. Assessment of compounds (**1–3** and **5, 6**) activity against the liver stage of *Plasmodium berghei* was also performed, measuring the luminescence intensity in Huh-7 cells infected with a firefly luciferase-expressing *P. berghei* line, PbGFP-Luc<sub>con</sub>. Active compounds were shown to inhibit the parasite's intracellular development rather than its ability to invade hepatic cells. Toxicity of compounds (**1–3** and **5, 6**) was assessed on the same cell line and on mouse primary hepatocytes through the fluorescence measurement of cell confluency. Furthermore, toxicity of compounds **1–6** towards human cells was also investigated in the MCF-7 breast cancer cell line, showing that they were not toxic or exhibited weak toxicity. In blood stages of *P. falciparum*, compounds **1–5** displayed antimalarial activity, revealing triacetyl balsaminol F (**5**) the highest antiplasmodial effects (IC<sub>50</sub> values: 0.4  $\mu$ M, 3D7; 0.2  $\mu$ M, Dd2). The highest antiplasmodial activity against the liver stages of *P. berghei* was also displayed by compound **5**, with high inhibitory activity and no toxicity.

© 2011 Elsevier Ltd. All rights reserved.

### 1. Introduction

Malaria is still a major global threat though some success exists in control programmes in several locations. It causes approximately 225 million incident infections per year, resulting in nearly one million deaths, 91% of which were in Africa. About 85% of the deaths occur in children under 5 years of age.<sup>1</sup> The disease is caused by protozoan parasites of the genus *Plasmodium*, and is transmitted by mosquitoes of the genus *Anopheles*. Among the five *Plasmodia* species affecting humans, *Plasmodium falciparum* is the most prevalent worldwide, particularly in Africa, causing the most severe form of the disease.<sup>1</sup>

In the absence of an effective vaccine, treatment and control of malaria is more complex due to the emergence of drug-resistant parasites. The spread of insecticide-resistant vectors of malaria is

also of great concern. To date, drug resistance has been reported in three malaria species known to affect humans, *P. falciparum*, *Plasmodium vivax* and *Plasmodium malariae*.<sup>2</sup> However, the increasing prevalence of drug-resistant *P. falciparum* strains represents the greatest challenge in malaria control. Therefore, in order to overcome drug-resistance, there is broad consensus that new antimalarial drugs, that exhibit antimalarial efficacy, are urgently needed. The discovery of new antimalarials by exploring natural products is considered of particular interest.<sup>3,4</sup> Natural product-derived compounds have played a major role in drug discovery and development.<sup>5–7</sup> In the case of malaria drug discovery, the great significance of plant-derived drugs for the treatment of the disease is highlighted by quinine, artemisinin and their derivatives, which are currently the mainstay of the antimalarial therapy.<sup>7</sup>

Most of the available antimalarial agents target blood stage parasites and only a limited number of drugs act on liver stages, the clinically silent stage that obligatorily precedes blood infection. In fact, presently, the only drug clinically approved by FDA against

\* Corresponding author. Tel.: +351 21 7946475; fax: +351 21 7946470.

E-mail address: [mjuferreira@ff.ul.pt](mailto:mjuferreira@ff.ul.pt) (M.-J.U. Ferreira).

*Plasmodium* liver stages, including dormant forms of the parasite, is the 8-aminoquinoline primaquine, which presents several adverse effects.<sup>8</sup> The study of *Plasmodium* liver stage development has been hampered by limitations in the experimental approaches required to quantify hepatocyte infection by the parasite. Therefore, the development of new drugs targeting *Plasmodium* liver stages represents an important and under-exploited site of intervention.<sup>9,10</sup>

*Momordica balsamina* L. (Cucurbitaceae), also referred to as the balsam apple, or African pumpkin, is an extensively cultivated vegetable consumed in many tropical and subtropical regions of the world.<sup>11,12</sup> It has also been widely used in traditional medicine in Africa to treat various diseases, mostly diabetes, and malaria symptoms.<sup>13–15</sup>

Bioassay-guided fractionation of the methanol extract of the aerial parts of *M. balsamina* led to the isolation of several cucurbitane-type triterpenoids with in vitro antimalarial activity against blood schizonts of chloroquine-sensitive and -resistant strains of *P. falciparum*.<sup>16,17</sup>

In this study, we report the isolation and structure elucidation of four cucurbitacins (**1–4**) from the same plant, two of which are new, along with two new ester derivatives (**5–6**). Compounds **1–6** were evaluated for their antimalarial activity against erythrocytic (blood) stages of *P. falciparum* (strains 3D7 and Dd2). Evaluation of the activity of compounds **1–3** and **5, 6** against liver stages of *P. berghei* infections was also carried out. The preliminary toxicity toward human cells of compounds **1–6** was also evaluated in the MCF-7 breast cancer cell line as well as in mouse primary hepatocytes.

## 2. Results and Discussion

### 2.1. Chemistry

The air-dried powdered aerial parts of *M. balsamina* were exhaustively extracted with methanol. Repeated bioassay-guided chromatographic fractionation and further HPLC purification of the ethyl acetate soluble fraction of the methanol extract yielded the new cucurbitane-type triterpenoids **1–2**. Acylation of compound **1** gave rise to the new triester derivatives, triacetyl balsaminol F, (**5**) and tribenzoyl balsaminol F (**6**). Known glycosylated cucurbitacins were also isolated. Their structures were assigned as cucurbita-5,24-diene-3 $\beta$ ,23(*R*)-diol-7-*O*- $\beta$ -D-glucopyranoside (**3**), and kuguaglycoside A (**4**) based on their spectroscopic data which were in good agreement with those described in the literature for these compounds.<sup>18,19</sup>

Compound **1**, named balsaminol F, was obtained as an amorphous powder with  $[\alpha]_D^{26} +122$  (c 0.12, MeOH). Its molecular formula was established as C<sub>30</sub>H<sub>50</sub>O<sub>3</sub>, based on the HR-ESI/MS data [M+Na]<sup>+</sup> at *m/z* 481.3649 (calcd. for C<sub>30</sub>H<sub>50</sub>O<sub>3</sub>Na 481.3652), indicating the presence of six degrees of unsaturation. The strong absorption band at 3396 cm<sup>-1</sup> in the IR spectrum of **1** revealed the presence of hydroxyl groups corroborated by NMR signals corresponding to oxygenated methine protons and carbons [ $\delta_H$  3.50 (br s),  $\delta_C$  77.5;  $\delta_H$  3.93 (br d, *J* = 5.2 Hz),  $\delta_C$  68.8;  $\delta_H$  4.41 (td, *J* = 9.6, 3.2)] (Table 1). Furthermore, the <sup>1</sup>H NMR spectrum of **1** displayed signals due to seven tertiary methyl groups as singlets at  $\delta_H$  0.74, 0.96, 1.03, 1.04, 1.18, 1.66, 1.69, and a secondary methyl as a doublet at  $\delta_H$  0.97 (*J* = 6.4 Hz). Vinylic NMR signals of two double bonds, at  $\delta_H$  5.16 (d, *J* = 8.5 Hz), and 5.74 (d, *J* = 5.1 Hz), were also found. The <sup>13</sup>C NMR spectrum (Table 1) of **1** revealed 30 carbon signals, which were assigned by a DEPT experiment as eight methyls, seven methylenes, nine methines (including three oxygenated and two vinylic), and six quaternary carbons (two sp<sup>2</sup>).

The above data indicated a tetracyclic triterpenic scaffold for **1** carrying two hydroxyl groups in addition to the characteristic hydroxyl at C-3. Detailed structural information was obtained from

**Table 1**  
<sup>1</sup>H (400 MHz), <sup>13</sup>C (150 MHz) NMR data for compounds **1** and **2**

Position	<b>1</b>		<b>2</b>	
	$\delta_C$	$\delta_H$ ( <i>J</i> in Hz)	$\delta_C^a$	$\delta_H$ ( <i>J</i> in Hz) <sup>b</sup>
1	22.4	1.57 m; 1.70 m	22.3	1.57 m; 1.70 m
2	30.1	1.71 m; 1.96 m	30.1	1.67 m; 1.97 m
3	77.5	3.50 br s	77.4	3.49 br s
4	42.3	–	42.4	–
5	148.3	–	148.7	–
6	122.5	5.74 d (5.1)	122.1	5.76 d (4.8)
7	68.8	3.93 br d (5.2)	74.4	4.11 br d (4.5)
8	54.1	1.98 br s	49.9	2.13 br s
9	35.0	–	35.1	–
10	40.1	2.32 br d (7.0)	40.1	2.34 br d (9.3)
11	33.9	1.51 m; 1.89 m	33.7	1.48 m; 1.70 m
12	31.5	1.54 m; 1.88 m	31.5	1.58 m; 1.69 m
13	47.2	–	47.3	–
14	49.5	–	49.2	–
15	35.7	1.31 m; 1.40 m	35.7	1.36 m
16	28.9	1.39 m; 1.70 m	28.8	1.40 m; 1.91 m
17	52.1	1.46 m	52.3	1.48 m
18	15.9	0.96 s	16.1	0.99 s
19	29.8	1.04 s	29.4	1.03 s
20	33.8	1.48 m	33.8	1.54 m
21	19.3	0.97 d (6.4)	19.3	0.98 d (7.2)
22	45.6	0.95 m; 1.63 m	45.7	1.82 m; 2.21 m
23	66.6	4.41 td (9.6, 3.2)	66.6	4.41 td (9.4, 2.8)
24	130.5	5.16 d (8.5)	130.5	5.16 d (8.4)
25	133.4	–	133.3	–
26	18.1	1.66 s	18.2	1.67 s
27	26.0	1.69 s	26.0	1.70 s
28	28.8	1.03 s	28.8	1.03 s
29	26.1	1.18 s	26.1	1.18 s
30	18.7	0.74 s	18.8	0.75 s

<sup>a</sup> <sup>13</sup>C NMR signals of 7-allose unit: 99.0 (C-1'), 72.3 (C-2'), 73.0 (C-3'), 69.1 (C-4'), 75.4 (C-5'), 63.2 (C-6').

<sup>b</sup> <sup>1</sup>H NMR signals of 7-allose unit: 4.75 (d, *J* = 8.0 Hz, H-1'), 3.32 (m, H-2'), 4.05 (br s, H-3'), 3.51 (m, H-4'), 3.66 (m, H-5'), 3.66 (m, H-6'), 3.84 (br d, *J* = 9.4 Hz, H-6').

the two-dimensional NMR data (<sup>1</sup>H–<sup>1</sup>H COSY, HMQC and HMBC–Fig. 1), which allowed the clear assignment of all the carbons and the location of the functional groups.

The relative stereochemistry of the tetracyclic nucleus of compound **1** was characterized by a NOESY experiment (Fig. 2), taking into account the coupling constants pattern of similar compounds and assuming an  $\alpha$  orientation for H-10, characteristic of cucurbitacins.<sup>20</sup> Concerning the side chain, the configuration at C-23 was assigned as *R*, mainly by comparison of the <sup>13</sup>C NMR data of the side chain carbons of **1** with those reported for a tetracyclic triterpene, which stereochemistry was established by X-ray

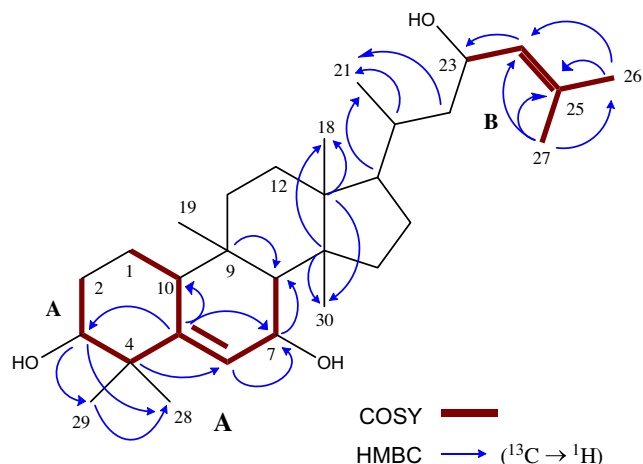


**Figure 1.** Key <sup>1</sup>H–<sup>1</sup>H COSY and HMBC correlations of compound **1**.

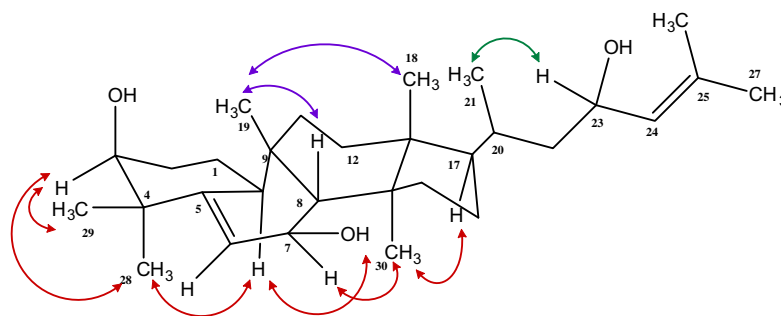


Figure 2. Key NOESY correlations of compound 1.

diffraction.<sup>21</sup> Identical configuration was previously found at C-23 in other cucurbitane derivatives isolated from the same plant.<sup>16,17,22</sup> Thus compound **1** was elucidated as cucurbita-5,24-diene-3 $\beta$ ,7 $\beta$ ,23(*R*)-triol.

Compound **2**, named balsaminoside B, was obtained as white crystals (mp 230–232 °C). Its molecular formula, C<sub>36</sub>H<sub>60</sub>O<sub>8</sub>, was established based on the pseudomolecular ion peak at *m/z* 643.4180 [M+Na]<sup>+</sup> in its HR-ESITOFMS data (calcd. for C<sub>36</sub>H<sub>60</sub>O<sub>8</sub>Na 643.4180). In the low resolution ESIMS spectrum of **2** was observed an ion at *m/z* 423 [M+H–H<sub>2</sub>O–C<sub>6</sub>H<sub>12</sub>O<sub>6</sub>]<sup>+</sup>, which suggested the presence of a sugar unit. Comparison of the <sup>1</sup>H and <sup>13</sup>C NMR spectra of **2** with those of compound **1** (Table 1), revealed six additional signals in the former, due to the sugar moiety. In the <sup>13</sup>C NMR spectrum of **2**, the signal corresponding to C-7 was shifted downfield ( $\Delta\delta_C = +5.6$ ), indicating that the sugar was located at this carbon. The heteronuclear <sup>3</sup>J<sub>C–H</sub> correlations observed in the HMBC spectrum confirmed this location. This structural feature was identified, unambiguously, as allose, a C-3 epimer of glucose, based on the equatorial configuration of H-3', revealed by a broad singlet at  $\delta_H$  4.05, due to small equatorial-axial couplings with the *vicinal* protons at C-2' and C-4'. In glucose, H-3' is axially oriented and appears as a triplet ( $J_{3ax,2ax} \cong J_{3ax,4ax} \cong 8,8$ ) as observed in compound **3**, and **4**. The <sup>3</sup>C NMR spectrum of **2** corroborated the above data.<sup>23,24</sup> The

relative stereochemistry of the nucleus of compound **2**, deduced from a NOESY experiment, was found to be identical to that of **1**. The configuration of the glycosidic linkage was determined as  $\beta$  based on the coupling constant value of the anomeric proton ( $J = 7.8$  Hz). From the above data, the structure of **2** was deduced as cucurbita-5,24-diene-3 $\beta$ ,23(*R*)-diol-7-*O*- $\beta$ -D-allopyranoside.

Acylation of balsaminol F (**1**) at C-3, C-7 and C-23, with acetic anhydride and benzoyl chloride, yielded the new triester derivatives, triacetylbalsaminol F, (**5**) and tribenzoylbalsaminol F (**6**), respectively (Fig. 3).

The molecular formula of the triester **5** was determined as C<sub>36</sub>H<sub>56</sub>NaO<sub>6</sub> by HR-ESITOFMS which showed a pseudomolecular ion at *m/z*: 607.3961 [M+Na]<sup>+</sup> (calcd. for C<sub>36</sub>H<sub>56</sub>NaO<sub>6</sub>Na 607.3969). Besides a molecular ion at *m/z* 584 [M]<sup>+</sup>, the EIMS spectrum of compound **5** exhibited ions at *m/z* 524 [M–CH<sub>3</sub>COOH]<sup>+</sup>, 464 [M–2 × CH<sub>3</sub>COOH]<sup>+</sup>, and 404 [M–3 × CH<sub>3</sub>COOH]<sup>+</sup>, resulting from the sequential loss of three acetyl groups, and its IR spectrum displayed absorption bands for ester carbonyls at 1729 and 1240 cm<sup>–1</sup>. These structural features were also evidenced by the NMR data of compound **5**, which revealed the presence of signals for three additional acetyl groups [ $\delta_H$  1.98 (6H, s), 1.96 (3H, s), Me-2', Me-2'', Me-2''');  $\delta_C$  170.5 (CO), 170.4 (CO), 170.3 (CO), 21.4, 21.2, and 21.1]. Moreover, when comparing the <sup>1</sup>H NMR spectrum

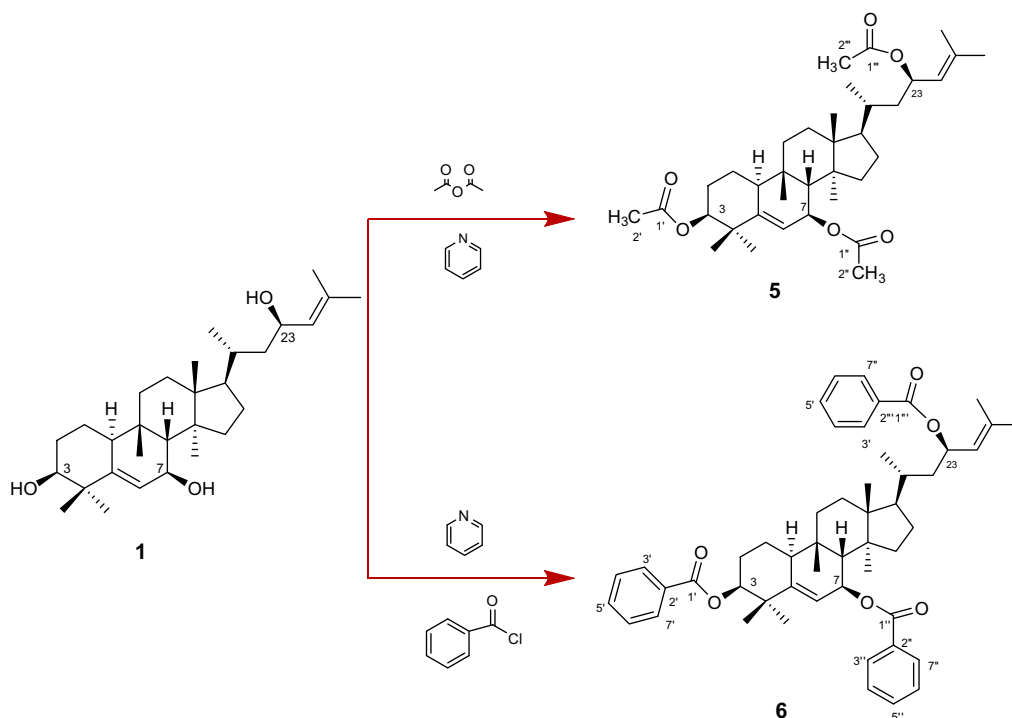


Figure 3. Acylation of Balsaminol F (**1**).

of compound **5** with that of compound **1**, the chemical shifts of the oxymethine protons H-3, H-7, and H-23 were shifted downfield by 1.22, 1.19 and 1.22 ppm, respectively. Significant paramagnetic effects were also observed in the signals of the  $^{13}\text{C}$  NMR spectrum, at the  $\alpha$ -carbons C-3, C-7, and C-23 and at the  $\gamma$ -carbons C-5 and C-25 and diamagnetic effects at the  $\beta$ -carbons C-2, C-4, C-6, C-8, C-22, and C-24. Similarly, acylation of balsaminol F (**1**) with benzoyl chloride afforded the new derivative tribenzoylbalsaminol F (**6**). The low resolution EIMS spectrum of **6** showed a molecular ion at  $m/z$  770  $[\text{M}]^+$  and the high resolution mass spectrum, HR-ESI-TOFMS, exhibited a pseudomolecular ion at  $m/z$ : 793.4438  $[\text{M}+\text{Na}]^+$  (calcd. for  $\text{C}_{51}\text{H}_{62}\text{NaO}_6\text{Na}$  793.4439). The NMR spectra of compound **6** provided evidence for the presence of three benzoyl ester residues. As above, when comparing the NMR data of compound **6** with that of the parent compound **1**, the most remarkable differences were found for proton and carbon resonances of rings A and B and side chain, namely for the carbons bearing the new ester functions and the corresponding geminal protons, which were shifted downfield, and also for the  $\alpha$ ,  $\beta$  and  $\gamma$ -carbons, as expected.

## 2.2. Biological activities

Compounds **1–6** were evaluated for their antimalarial activity against chloroquine-sensitive (3D7) and resistant (Dd2) *P. falciparum* strains, using a standardized SYBR Green I-based fluorescence assay.<sup>25,26</sup> Chloroquine was used as positive control and the effects of compounds against both strains were expressed as  $\text{IC}_{50}$  values in  $\mu\text{M}$  and  $\mu\text{g}/\text{mL}$ . These results, as well as the compounds' cytotoxic activity against breast cancer cells (MCF-7) and their selectivity index (SI) are summarized in Table 2. A great diversity of criteria has been adopted for assessing in vitro antimalarial activity of pure compounds. In accordance with literature data,<sup>27</sup> the antimalarial activity of the compounds described in this work was defined as:  $\text{IC}_{50} \leq 1 \mu\text{M}$ , excellent/potent activity;  $1 < \text{IC}_{50} \leq 10 \mu\text{M}$ , good activity; and  $10 < \text{IC}_{50} \leq 30 \mu\text{M}$ , moderate activity. Compounds with an  $\text{IC}_{50} > 30 \mu\text{M}$  were considered inactive. Therefore, compounds **1–5** displayed antimalarial activity (Table 2) and compound **6** was inactive. Among the isolated compounds, the glycoside derivatives (**2–4**) revealed a good antimalarial activity against both strains tested (**2**,  $\text{IC}_{50} = 2.9$  and  $6.3 \mu\text{M}$ , for 3D7 and Dd2, respectively; **3**,  $\text{IC}_{50} = 3.4$  and  $7.2 \mu\text{M}$ , for 3D7 and Dd2, respectively; **4**,  $\text{IC}_{50} = 3.9$  and  $4.7 \mu\text{M}$ , for 3D7 and Dd2, respectively), suggesting that the sugar unit plays a role in the antiplasmodial activity. However, as shown in Table 2, the acylated derivative triacetylbalsaminol F displayed the strongest antiplasmodial activity, being 22.5- ( $\text{IC}_{50} = 0.8 \mu\text{M}$  for 3D7) and 50-fold ( $\text{IC}_{50} = 0.4 \mu\text{M}$ , for Dd2) more active than the parent compound, balsaminol F (**1**,  $\text{IC}_{50} = 18.0$  and  $20.0 \mu\text{M}$  for 3D7 and Dd2, respectively), against the sensitive and resistant strains, respectively. These  $\text{IC}_{50}$  values are comparable with those obtained with chloroquine, particularly against the resistant Dd2 strain ( $\text{IC}_{50} = 0.016$  and  $0.20 \mu\text{M}$  for 3D7 and Dd2,

respectively). Conversely, it is interesting to stress that the activity was lost when the acetyl groups at positions C-3, C-7, and C-23 of compound **5** were replaced by benzoyl groups in the benzoylated derivative, tribenzoylbalsaminol F (**6**), which was inactive against both strains ( $\text{IC}_{50} = 57.3$  and  $68.4 \mu\text{M}$  for 3D7 and Dd2, respectively).

As can be observed in Table 2, the isolated compounds (**1–4**) showed low toxicity ( $\text{IC}_{50}$  14.2–27.3  $\mu\text{M}$ ) against the MCF-7 human breast cancer cell line. However, a low selectivity index (SI) was found (SI <7.0). On the other hand, no cytotoxic activity ( $\text{IC}_{50} > 133.3 \mu\text{M}$ ) was exhibited by both balsaminol F (**1**) derivatives (**5**, **6**). More importantly, a high SI value was found for triacetylbalsaminol F (**5**) (SI >162.4 and 342.9 for 3D7 and Dd2 *P. falciparum* strains, respectively).

Compounds **1–3**, **5** and **6** were also evaluated for their activity against liver stages of the rodent malaria parasite *P. berghei*, at 1, 5 and 15  $\mu\text{M}$ , using a recently described bioluminescence-based method. This method employs a transgenic *P. berghei* parasite, PbGFP-Luc<sub>con</sub>, expressing the bioluminescent reporter protein luciferase to visualize and quantify parasite development in Huh-7 cells, a human hepatoma cell line.<sup>9</sup> (Fig. 4-bars). Primaquine was used as positive control. Moreover, toxicity of compounds (**1–3**, **5** and **6**) was also assessed on the same cell line (Fig. 4-line) and on mouse primary hepatocytes (Fig. 5) through the fluorescence measurement of cell confluency. As can be observed, all the compounds tested in this model exhibited significant in vitro activity against *P. berghei* liver stages (Fig. 4). However, balsaminol F (**1**) and, in particular, balsaminoside B (**2**) displayed significant toxicity against Huh-7 cells and mouse primary hepatocytes at 15  $\mu\text{M}$  (Fig. 4-line, Fig. 5). Interestingly, balsaminoside B (**2**), which displays a rare allose (C-3' glucose epimer) sugar at C-7, showed superior anti-*Plasmodium* activity when compared with the glucose analogue (**3**) thus demonstrating that activity is sugar-dependent. As observed for the relative activities of the compounds against the parasite's blood stages, triacetylbalsaminol F (**5**) showed the most potent inhibitory activity against the liver stages of *Plasmodium*, displaying higher activity than primaquine, with no detectable toxicity towards the cells assayed, at the concentrations employed (Fig. 4 and Fig. 5). Further investigation is warranted in order to elucidate its mechanism of action.

To assess whether the liver stage activity exhibited by the compounds is due to their action on parasite motility and invasion, or on intracellular parasite development, the effect of adding the compounds prior to parasite addition was compared with the effect of adding compounds after invasion of the cells by the parasites had been completed. In this infection system, invasion is >95% complete within 2 h of sporozoite addition to the cells.<sup>10</sup> Therefore, any effects of compounds added after that time point on overall infection, as measured by the luciferase-based assay employed, are not due to the compounds acting on parasite motility or invasion, but rather on intracellular liver stages. Our data indicate

**Table 2**  
In vitro antimalarial activity against *P. falciparum* 3D7, and Dd2 strains, cytotoxicity, and selectivity index and resistance index of compounds **1–6**

Compounds	$\text{IC}_{50} \pm \text{SD}$				MCF7 cells $\mu\text{M}$	SI	
	<i>P. falciparum</i> 3D7		<i>P. falciparum</i> Dd2			MCF7/3D7	MCF7/Dd2
	$\mu\text{M}$	$\mu\text{g}/\text{mL}$	$\mu\text{M}$	$\mu\text{g}/\text{mL}$			
Balsaminol F ( <b>1</b> )	18.0 $\pm$ 1.7	8.2 $\pm$ 0.8	20.0 $\pm$ 4.3	9.2 $\pm$ 2.0	27.3 $\pm$ 1.2	1.5	1.4
Balsaminoside B ( <b>2</b> )	2.9 $\pm$ 0.1	1.8 $\pm$ 0.1	6.3 $\pm$ 0.7	3.9 $\pm$ 0.4	14.2 $\pm$ 0.8	4.8	2.3
Balsaminoside C ( <b>3</b> )	3.4 $\pm$ 0.6	2.1 $\pm$ 0.3	7.2 $\pm$ 0.4	4.5 $\pm$ 0.3	23.9 $\pm$ 6.6	7.0	3.3
Kuguaglycoside A ( <b>4</b> )	3.9 $\pm$ 0.4	2.5 $\pm$ 0.2	4.7 $\pm$ 0.4	2.9 $\pm$ 0.2	13.5 $\pm$ 4.9	3.5	2.9
Triacetylbalsaminol F ( <b>5</b> )	0.8 $\pm$ 0.1	0.5 $\pm$ 0.1	0.4 $\pm$ 0.04	0.2 $\pm$ 0.02	>133.3	>162.4	>342.9
Tribenzoylbalsaminol F ( <b>6</b> )	57.3 $\pm$ 3.1	44.2 $\pm$ 2.4	68.4 $\pm$ 8.6	52.7 $\pm$ 6.7	>133.3	>2.3	>2.0
Chloroquine	0.016		0.2				

Values shown are the mean  $\text{IC}_{50} \pm \text{SD}$  ( $\mu\text{M}$ ) from three independent experiments. Selectivity index (SI) is defined as the ratio of cytotoxicity ( $\text{IC}_{50}$ ) to antiplasmodial activity ( $\text{IC}_{50}$ ).

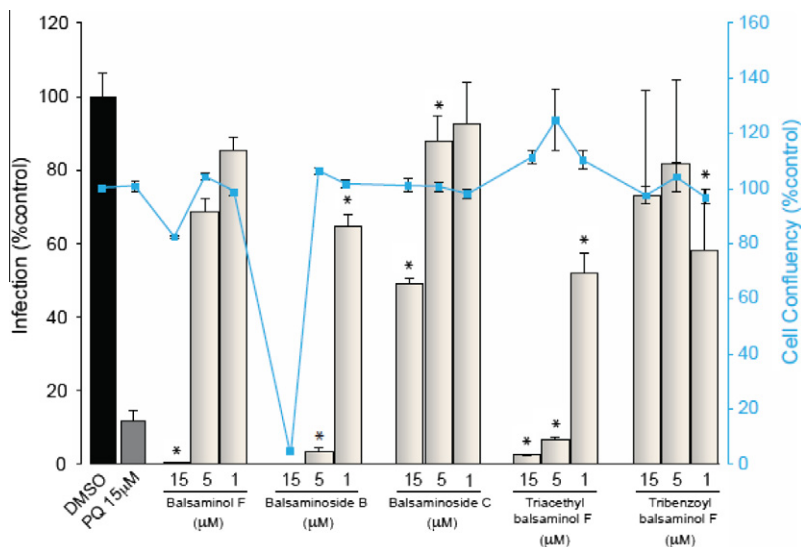


**Figure 4.** Drug inhibition of liver stage infection, determined by measurement of luciferase activity (bars), and compound toxicity, assessed by fluorescence measurement of cell confluency (line), in *PbGFP-Luc<sub>cont</sub>*-infected Huh-7. PQ-primaquine, used as positive control. DMSO- solvent-treated control. Error bars represent the standard deviations of three independent measurements. (\**p* < 0.05; paired student's test calculated relative to DMSO controls).

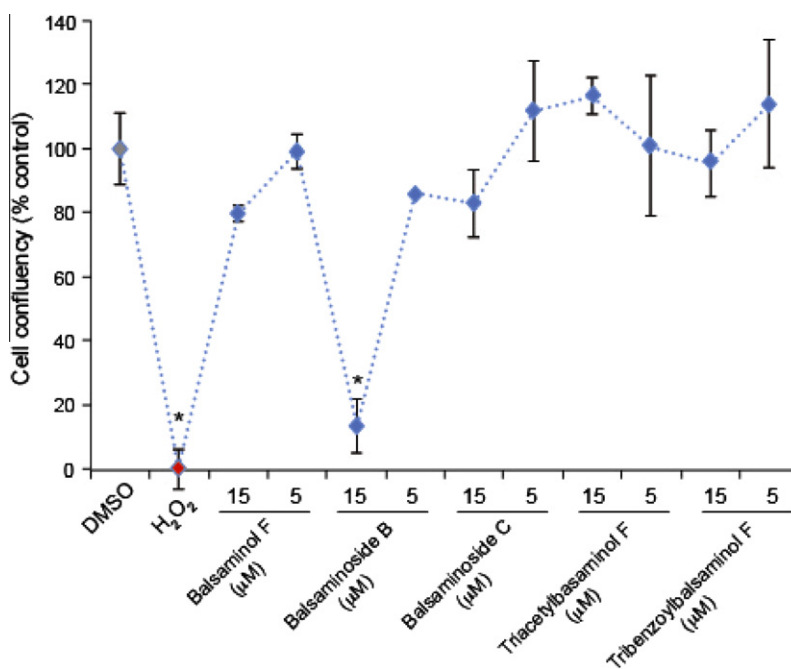


**Figure 5.** Cytotoxicity activity of compounds (1–3 and 5–6) in mouse primary hepatocyte cells assessed by fluorescence measurement of cell confluency. H<sub>2</sub>O<sub>2</sub> (500 µM) and cells incubated with an amount of DMSO equivalent to that present in the highest drug concentrations were used as positive and negative controls, respectively. (\**p* < 0.05; paired student's test calculated relative to DMSO).

that balsaminol F (1), balsaminoside B (2) and triacetyl balsaminol F (5), the most active compounds (Fig. 4), do act on the parasite's intracellular liver stages and have little or no influence on parasite motility/invasion (Fig. 6).

### 3. Experimental Section

#### 3.1. Chemistry

##### 3.1.1. General Experimental Procedures

Optical rotations were obtained using a Perkin Elmer 241 polarimeter. IR spectra were determined on a FTIR Nicolet Impact 400, and NMR spectra recorded on a Bruker ARX-400 NMR spectrom-

eter (<sup>1</sup>H 400 MHz; <sup>13</sup>C 100.61 MHz), using CD<sub>3</sub>OD and acetone as solvent. ESIMS were taken on a Micromass Quattro micro API and HR-ESITOFMS on a Bruker-Microtof ESITOF (Biotof II Model, Bruker) and on a Bruker Daltonics maXis (ESI/NanoSpray-Qq-TOF). EIMS, HR-EIMS, HR-CIMS were recorded on a Micromass Autospec spectrometer. TLC was performed on precoated SiO<sub>2</sub> F<sub>254</sub> plates (Merck 5554 and 5744), with visualization under UV light and by spraying with sulfuric acid-methanol (1:1), followed by heating. Column chromatography (CC) was carried out on silica gel (Merck 9385). TLC were performed on precoated silica gel F<sub>254</sub> plates (Merck 5554 and 5744) and visualized under UV light and by spraying sulfuric acid-methanol (1:1) followed by heating. HPLC was carried out on a Merck-Hitachi instrument, with UV detection

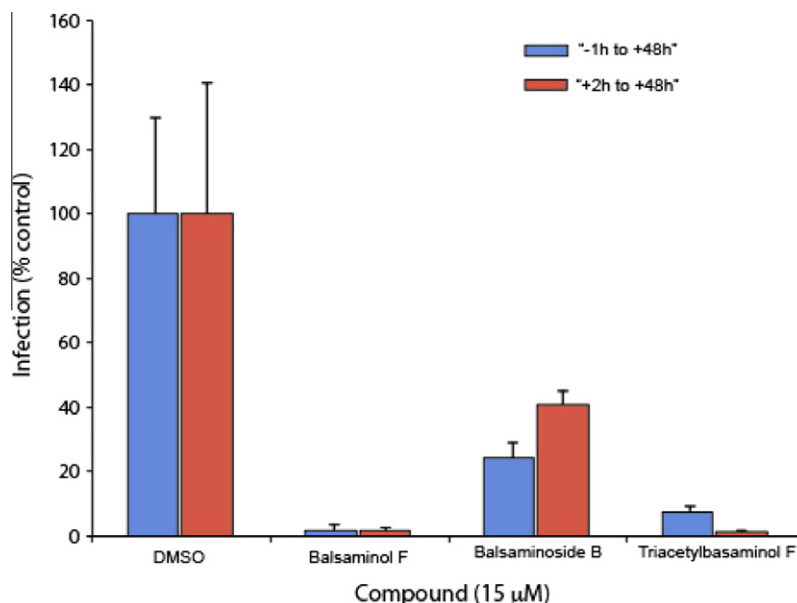


**Figure 6.** Comparison of the effect of adding the active compounds (**1**, **2** and **5**) prior to parasite addition, with that of adding them after invasion of the cells by the parasites.

(210 and 220 nm), using a Merck LiChrospher 100 RP-18 (10 μm, 250 × 10 mm) column.

### 3.1.2. Extraction and Isolation

Dried aerial parts of *Momordica balsamina* (1.2 kg) were powdered and exhaustively extracted with methanol (11 × 8 L) at room temperature, as previously described.<sup>28</sup> Briefly, the MeOH extract was evaporated to afford a residue (280 g), which was suspended in H<sub>2</sub>O (1 L) and extracted with EtOAc (9 × 0.5 L). The EtOAc residue (85 g) was suspended in MeOH/H<sub>2</sub>O (9:1; 1 L), and extracted with *n*-hexane (5 × 0.5 L) for removal of waxy material that was not further studied. The remaining extract was evaporated under vacuum (40 °C), yielding a residue (45 g) that was chromatographed over silica gel (1 kg), using mixtures of *n*-hexane/EtOAc (1:0 to 0:1) and EtOAc/MeOH (19:1 to 0:1) as eluents to obtain six fractions (Fr 1–6), which were combined according to TLC analysis. Fr 2 (2.1 g), eluted with a mixture of *n*-hexane/EtOAc (1:1), was chromatographed with mixtures of *n*-hexane/EtOAc. A sub-fraction (372 mg) was fractionated by repeated column chromatography with mixtures of CH<sub>2</sub>Cl<sub>2</sub>/acetone. A final purification was carried out by HPLC to afford 50 mg of compounds **1**. The crude Fr 5 (2.8 g), eluted with mixtures of *n*-hexane/EtOAc (1:1 to 0:1) and EtOAc/MeOH (1:0 to 1:1), was repetitively fractionated by column chromatography yielding a sub-fraction, which was further purified by HPLC to afford 7 mg of compound **4**. The residue (11.9 g) of Fr 6 (EtOAc/MeOH, 93:7 to 9:1) was recrystallized from EtOAc/MeOH to give 500 mg of a mixture, which was fractionated by column chromatography (SiO<sub>2</sub>, 50 g), eluted with mixtures of *n*-hexane/EtOAc (3:1 to 1:0) and EtOAc/MeOH (1:0 to 1:1). The fractions eluted with EtOAc/MeOH (97:3) were evaporated and recrystallized, from *n*-hexane/EtOAc, to afford 160 mg of compound **2**. The mother liquors were associated to the remaining fractions and after evaporation, the residue (245 mg) was submitted to repeated column chromatography, using as eluents mixtures of EtOAc/MeOH, and CH<sub>2</sub>Cl<sub>2</sub>/MeOH of increasing polarity, to afford more 110 mg of compound **2** and 11 mg of compound **3**.

**3.1.2.1. Balsaminol F, cucurbita-5,24-diene-3β,7β,23(R)-triol (1).** Amorphous, white powder;  $[\alpha]_D^{26} + 122$  (c 0.12, MeOH); IR (KBR)  $\nu_{\max}$  3396, 2936, 1645, 1459, 1389, 939 cm<sup>-1</sup>; <sup>1</sup>H and

<sup>13</sup>C NMR data, see Table 1; ESIMS  $m/z$ : 939 [2M+Na]<sup>+</sup> (20), 481 [M+Na]<sup>+</sup> (21); HR-ESITOFMS  $m/z$ : 481.3649 [M+Na]<sup>+</sup> (calcd. for C<sub>30</sub>H<sub>50</sub>O<sub>3</sub>Na 481.3652).

**3.1.2.2. Balsaminoside B, cucurbita-5,24-diene-3β,23(R)-diol-7-O-β-D-allopyranoside (2).** Prismatic white crystals mp: [230–231 °C (*n*-hexane/EtOAc)];  $[\alpha]_D^{26} + 173$  (c 0.11, MeOH); IR (KBR)  $\nu_{\max}$  3396, 2945, 1645, 1453, 1383, 1057, 978, 939 cm<sup>-1</sup>; <sup>1</sup>H and <sup>13</sup>C NMR data, see Table 1; ESIMS  $m/z$ : 659 [M+K]<sup>+</sup> (4), 643 [M+Na]<sup>+</sup> (100), 423 [M+H-H<sub>2</sub>O-C<sub>6</sub>H<sub>12</sub>O<sub>6</sub>]<sup>+</sup> (10); HR-ESITOFMS  $m/z$ : 643.4180 [M+Na]<sup>+</sup> (calcd. for C<sub>36</sub>H<sub>60</sub>O<sub>8</sub>Na 643.4180).

### 3.1.3. Preparation of balsaminol F esters

**3.1.3.1. Acetylation with acetic anhydride.** Compound **1** (10 mg) was suspended in acetic anhydride (1 mL) and pyridine (1 mL). After stirring at room temperature overnight, the excess of reagents was eliminated with N<sub>2</sub> and the product obtained was purified by column chromatography (*n*-hexane/EtOAc, 4:1) to afford 10 mg of compound **5**.

**3.1.3.1.1. Triacetylbasaminol F, 3β,7β,23(R)-triacetoxycucurbita-5,24-diene (5).** Colorless oil; IR (KBR)  $\nu_{\max}$  1729, 1528, 1462, 1370, 1240, 1015, 987, 827, 611 cm<sup>-1</sup>; EIMS,  $m/z$  (rel. int.): 584 [M]<sup>+</sup> (<1), 524 [M-CH<sub>3</sub>COOH]<sup>+</sup> (27), 482 (100), 464 [M-2 × CH<sub>3</sub>COOH]<sup>+</sup> (10), 421 (11), 404 [M-3 × CH<sub>3</sub>COOH]<sup>+</sup> (4); HR-ESITOFMS  $m/z$ : 607.3961 [M+Na]<sup>+</sup> (calcd. for C<sub>36</sub>H<sub>56</sub>NaO<sub>6</sub>Na 607.3969); <sup>1</sup>H NMR (400 MHz, CD<sub>3</sub>COCD<sub>3</sub>): δ 5.67 (1H, d, J = 4.8 Hz, H-6), 5.63 (1H, td, J = 8.8, 3.2 Hz, H-23), 5.12 (2H, m, H-7/H-24), 4.72 (1H, br d, J = 12.0 Hz, H-10), 1.98 and 1.96 (6H and 3H, s, Me-2'/Me-2''/Me-2'''), 1.97 (3H, br s, H-8), 1.71 (3H, s, Me-27), 1.68 (3H, s, Me-26), 1.14 (3H, s, Me-28), 1.09 (3H, s, Me-29), 1.01 (3H, s, Me-19), 0.96 (3H, d, J = 6.0 Hz, Me-21), 0.88 (3H, s, Me-18), 0.82 (3H, s, Me-30); <sup>13</sup>C NMR (101 MHz, CD<sub>3</sub>COCD<sub>3</sub>): δ 170.5, 170.4, 170.3 (C-1'/C-1''/C-1'''), 150.0 (C-5), 135.7 (C-25), 125.9 (C-24), 118.5 (C-6), 79.0 (C-3), 70.8 (C-7), 69.4 (C-23), 51.4 (C-8), 51.1 (C-17), 49.0 (C-14), 46.8 (C-13), 42.7 (C-22), 40.8 (C-4), 39.3 (C-10), 35.3 (C-15), 34.6 (C-9), 33.6 (C-20), 33.0 (C-11), 30.8 (C-12), 29.0 (C-19), 28.6 (C-16), 28.4 (C-28), 27.0 (C-2), 25.7 (C-27), 25.2 (C-29), 22.4 (C-1), 21.4, 21.2, 21.1 (C-1'/C-1''/C-1'''), 19.3 (C-21), 18.5 (C-26), 18.4 (C-30), 15.7 (C-18).

**3.1.3.2. Acylation with benzoyl chloride.** Compound **1** (17.6 mg) was suspended in benzoyl chloride (1 mL) and pyridine (1 mL). After stirring at room temperature overnight, the excess of pyridine was eliminated as above and the product obtained was purified by column chromatography (*n*-hexane/EtOAc, 1:0 to 4:1). Further purification by preparative TLC (*n*-hexane/EtOAc, 9:1) afforded 17 mg of compound **6**.

**3.1.3.1.2. Tribenzoylbalsaminol F, 3 $\beta$ ,7 $\beta$ ,23(R)-tribenzoyloxycurcubita-5,24-diene (6).** Colorless oil; IR (KBR)  $\nu_{\text{max}}$  1718, 1528, 1462, 1370, 1240, 1015, 836, 870, 719  $\text{cm}^{-1}$ ; EIMS, *m/z* (rel. int.): 770 [M]<sup>+</sup> (<1), 526 [M-2  $\times$  C<sub>6</sub>H<sub>5</sub>COOH]<sup>+</sup> (26.7); HR-ESITOFMS *m/z*: 793.4438 [M+Na]<sup>+</sup> (calcd. for C<sub>51</sub>H<sub>62</sub>NaO<sub>6</sub>Na 793.4439); <sup>1</sup>H NMR (400 MHz, CD<sub>3</sub>COCD<sub>3</sub>):  $\delta$  8.10–7.99 (6H, m, H-3'/H-3''/H-3'''/H-7'/H-7''/H-7'''), 7.70–7.37 (9H, m, H-4'/H-4''/H-4'''/H-5'/H-5''/H-5'''/H-6'/H-6''/H-6'''), 5.92 (2H, m, m, H-6/H-23), 5.50 (1H, brd, *J* > 5.6 Hz, H-7), 5.29 (1H, d, *J* = 8.8 Hz, H-24), 5.02 (1H, br s, H-3), 2.69 (1H, br d, *J* = 12.4 Hz, H-10), 2.16 (1H, br s, H-8), 1.83 (3H, s, Me-26), 1.73 (3H, s, Me-27), 1.27 (3H, s, Me-28), 1.25 (3H, s, Me-19), 1.21 (3H, s, Me-29), 1.06 (3H, d, *J* = 5.2 Hz, Me-21), 0.97 (3H, s, Me-18), 0.88 (3H, s, Me-30); <sup>13</sup>C NMR (101 MHz, CD<sub>3</sub>COCD<sub>3</sub>):  $\delta$  166.0, 165.8, 165.5 (C-1'/C-1''/C-1'''), 150.5 (C-5), 136.2 (C-25), 133.6, 133.5 (C-5'/C-5''/C-5'''), 131.9, 131.6, 131.5 (C-2'/C-2''/C-2'''), 129.9, 129.8 (C-3'/C-3''/C-3'''/C-7'/C-7''/C-7'''), 129.3, 129.2 (C-4'/C-4''/C-4'''/C-6'/C-6''/C-6'''), 125.5 (C-24), 118.6 (C-6), 79.9 (C-3), 71.3 (C-7), 70.2 (C-23), 51.2 (C-8), 50.9 (C-17), 48.9 (C-14), 46.7 (C-13), 42.6 (C-22), 41.3 (C-4), 38.9 (C-10), 35.2 (C-15), 34.5 (C-9), 33.6 (C-20), 32.9 (C-11), 30.6 (C-12), 29.7 (C-19), 28.6 (C-16), 27.2 (C-28), 26.4 (C-2), 25.6 (C-27), 25.5 (C-28), 22.4 (C-1), 19.2 (C-21), 18.4 (C-30), 18.5 (C-26), 15.7 (C-18).

## 3.2. Biological assays

### 3.2.1. In vitro cytotoxicity assay

Human breast cancer MCF-7 cell line was cultured in RPMI 1640 medium supplemented with 10% heat inactivated horse serum, L-glutamine (2 mM), and antibiotics, in a humidified atmosphere of 5% CO<sub>2</sub> at 37 °C. The effects of increasing concentrations of compounds on cell growth were tested in 96-well flat-bottomed microtiter plates. The compounds were diluted in a volume of 50  $\mu$ L medium. Then, 2  $\times$  10<sup>4</sup> cells in 0.1 mL of medium were added to each well, with the exception of the medium control wells. The culture plates were further incubated at 37 °C for 24 h. At the end of the incubation period, 15  $\mu$ L of MTT (thiazolyl blue, Sigma, St Louis, MO, USA) solution (from a 5 mg/mL stock) was added to each well. After incubation at 37 °C for 4 h, 100  $\mu$ L of sodium dodecyl sulfate (SDS) (Sigma, St Louis, MO, USA) solution (10%) was measured into each well and the plates were further incubated at 37 °C overnight. The cell growth was determined by measuring the optical density (OD) at 550 nm (ref. 630 nm) with a Dynatech MRX vertical beam ELISA reader. Inhibition of cell growth (as a percentage) was determined according to the formula:

$$100 - \left[ \frac{\text{OD sample} - \text{OD medium control}}{\text{OD cell control} - \text{OD medium control}} \right] \times 100$$

Where IC<sub>50</sub> is defined as the inhibitory dose that reduces the growth of the compound-exposed cells by 50%. The IC<sub>50</sub> values are expressed as means  $\pm$  SD from three experiments.

Compound toxicity on mouse primary hepatocytes was evaluated by determining cell confluence following incubation with the compounds. Briefly, cells were incubated with the compounds for 24 h and further incubated for 1 h with AlamarBlue-containing medium prior to fluorescence measurement. Fluorescence was normalized to that of cells incubated with 500  $\mu$ M H<sub>2</sub>O<sub>2</sub>, used as a positive control in the assay, and compared with that of cells incubated with an amount equivalent to that present in the highest drug concentrations.

### 3.2.2. In vitro antimalarial activity in human red blood cells

Human malaria parasites were cultured as previously described by Trager and Jensen (1976), with minor modifications.<sup>29</sup> Briefly, 3D7 and Dd2 *Plasmodium falciparum* strains were cultivated in recently collected erythrocytes as host cells in RPMI 1640 medium (Gibco) containing 25 mM HEPES (Sigma) and 6.8 mM hypoxanthine (Sigma) supplemented with 10% AlbuMAX II (Invitrogen). Cultures were maintained at 37 °C under an atmosphere of 5% O<sub>2</sub>, 3–5% CO<sub>2</sub>, and N<sub>2</sub>. The antimalarial activity of the compounds was determined by a fluorometric method using SYBR Green I.<sup>24,25</sup> In brief, stock solutions of the samples were prepared in DMSO (10 mg/mL), and were diluted to give a series of concentrations ranging from 0.156 to 100  $\mu$ g/mL. 50  $\mu$ L of each testing concentration, together with 50  $\mu$ L of a 1% red blood parasitized cell suspension with ring stages and 2% haematocrit were distributed in duplicate, into each of the 96-well plates. Plates were incubated for 48 h at 37 °C. After, 100  $\mu$ L of SYBR Green I in lysis buffer (Tris 20 mM; pH 7.5, EDTA-5 mM, saponin-0.008%; wt/vol, Triton X-100-0.08%; vol/vol, and 0.2  $\mu$ L of SYBR Green I/ml of lysis buffer) was added to each well. Plates were covered, mixed and incubated in the dark at room temperature for 1 h. Fluorescence intensity was measured on a fluorescence multiwell plate reader, Anthos venyht 3100 (Alfagene) excitation and emission wavelengths of 485 and 535 nm, respectively. Values were expressed in relative fluorescence units. Analysis of the results obtained and IC<sub>50</sub> determination were performed with HN-NonLineV1.1 (H. Noedl, 2001) software.

### 3.2.3. In vitro anti-Plasmodium liver stage activity

Huh-7 cells, a human hepatoma cell line, were cultured in RPMI 1640 medium supplemented with 10% v/v fetal calf serum (FCS), 1% v/v non-essential amino acids, 1% v/v penicillin/streptomycin, 1% v/v glutamine and 10 mM 4-(2-hydroxyethyl)-1-piperazineethanesulphonic acid (HEPES), pH 7, and maintained at 37 °C with 5% CO<sub>2</sub>. Huh-7 cells (12  $\times$  10<sup>3</sup> per well) were seeded in 96-well plates the day before drug treatment and infection. Inhibition of liver stage infection was determined by measuring the luminescence intensity in Huh-7 cells infected with a firefly luciferase-expressing *P. berghei* line, *PbGFP-Luc<sub>con</sub>*, as previously described.<sup>9</sup> Compounds were added 1 h prior to addition of sporozoites freshly obtained through disruption of salivary glands of infected female *Anopheles stephensi* mosquitos. Sporozoite addition was followed by centrifugation at 1700g for 5 min. Inhibition of parasite development was measured 48 h after infection. The effect of the compounds on the viability of Huh-7 cells was assessed by measuring AlamarBlue fluorescence (Invitrogen, UK), using the manufacturer's protocol.

## Acknowledgment

This study was supported by FCT, Portugal (BD/22321/2005 to Cátia Ramalheite and SFRH/BPD/64539/2009 to Filipa P. da Cruz). The authors thank Dr. Teresa Vasconcelos, Instituto Superior de Agronomia, Universidade de Lisboa, Portugal for the taxonomic work on the plant material, and also Dr. Catarina Arruda from the Portuguese Embassy in Mozambique, as well as the Portuguese Office of International Affairs for plant transport.

## Supplementary data

Supplementary data (1D and 2D NMR spectra of compounds **1–12**) associated with this article can be found, in the online version, at doi:10.1016/j.bmc.2011.10.044.

## References and notes

- WHO, World Malaria Report; Geneve, Switzerland, 2010.
- WHO, Global report on antimalarial drug efficacy and drug resistance: 2000–2010; Geneve, Switzerland, 2008.

3. Grimberg, B. T.; Mehlotra, R. K. *Pharmaceuticals* **2011**, *4*, 681.
4. Guantai, E.; Chibale, K. *Malar. J.* **2011**, *10*, S2.
5. Newman, D. J.; Cragg, G. M. *J. Nat. Prod.* **2007**, *70*, 461.
6. Newman, D. J. *J. Med. Chem.* **2008**, *51*, 2589.
7. Butler, M. S.; Newman, D. J. *Prog. Drug Res.* **2008**, *65*, 3.
8. Wells, T. N.; Burrows, J. N.; Baird, J. K. *Trends Parasitol.* **2010**, *26*, 145.
9. Ploemen, I. H.; Prudêncio, M.; Douradinha, B. G.; Ramesar, J.; Fonager, J.; van Gemert, G. J.; Luty, A. J.; Hermsen, C. C.; Sauerwein, R. W.; Baptista, F. G.; Mota, M. M.; Waters, A. P.; Que, I.; Lowik, C. W.; Khan, S. M.; Janse, C. J.; Franke-Fayard, B. M. *PLoS One.* **2009**, *4*, e7881.
10. Prudencio, M.; Rodrigues, C. D.; Ataide, R.; Mota, M. M. *Cell Microbiol.* **2008**, *10*, 218.
11. Flyman, M. V.; Afolayan, A. J. *Int. J. Food Sci. Nutr.* **2007**, *58*, 419.
12. Thakur, G. S.; Bag, M.; Sanodiya, B. S.; Bhadauriya, P.; Debnath, M.; Prasad, G.; Bisen, P. S. *Cur. Pharm. Bio.* **2009**, *10*, 667.
13. van de Venter, M.; Roux, S.; Bungu, L. C.; Louw, J.; Crouch, N. R.; Grace, O. M.; Maharaj, V.; Pillay, P.; Sewnarian, P.; Bhagwandin, N.; Folb, P. J. *Ethnopharmacol.* **2008**, *119*, 81.
14. Bandeira, S. O.; Gaspar, F.; Pagula, F. P. *Pharm. Biol.* **2001**, *39*, 70.
15. Geidam, M. A. D. E.; Hamza, H. G. *Pakistan J. Biol. Sci.* **2004**, *7*, 397.
16. Ramalhete, C.; Lopes, D.; Mulhovo, S.; Molnar, J.; Rosario, V. E.; Ferreira, M. J. U. *Bioorg. Med. Chem.* **2010**, *18*, 5254.
17. Ramalhete, C.; Lopes, D.; Mulhovo, S.; Molnar, J.; Rosario, V. E.; Ferreira, M. J. U. *Bioorg. Med. Chem.* **2011**, *19*, 330.
18. Fatope, M. O.; Takeda, Y.; Yamashita, H.; Okabe, H.; Yamauchi, T. *J. Nat. Prod.* **1990**, *53*, 1491.
19. Chen, J. C.; Lu, L.; Zhang, X. M.; Zhou, L.; Li, Z. R.; Qiu, M. H. *Helv. Chim. Acta* **2008**, *91*, 920.
20. Xu, R.; Fazio, G. C.; Matsuda, S. P. T. *Phytochemistry* **2004**, *65*, 261.
21. Cantrell, C. L.; Lu, T.; Fronczek, F. R.; Fischer, H. J. *J. Nat. Prod.* **1996**, *59*, 1131.
22. Ramalhete, C.; Mansoor, T. A.; Mulhovo, S.; Molnar, J.; Ferreira, M. J. U. *J. Nat. Prod.* **2009**, *72*, 2009.
23. Qing-Yan, L.; Hu-Biao, C.; Zhen Ming, L.; Bin, W.; Yu-Ying, Z. *Magn. Reson. Chem.* **2007**, *45*, 451.
24. Liu, X.; Cui, Y.; Yu, Q.; Yu, B. *Phytochemistry* **2005**, *66*, 1671.
25. Johnson, J. D.; Dennon, R. A.; Gerena, L.; Lopez-Sanchez, M.; Roncal, N. E.; Waters, N. C. *Antimicrob. Agents Chemother.* **2007**, *51*, 1926.
26. Smilkstein, M.; Sriwilaijaroen, N.; Kelly, J. X.; Wilairat, P.; Riscoe, M. *Antimicrob. Agents Chemother.* **2004**, *48*, 1803.
27. Batista, R.; Silva, A. D.; de Oliveira, A. B. *Molecules* **2009**, *14*, 3037.
28. Ramalhete, C.; Molnar, J.; Mulhovo, S.; Rosario, V. E.; Ferreira, M. J. U. *Bioorg. Med. Chem.* **2009**, *17*, 6942.
29. Trager, W.; Jensen, J. B. *Science* **1976**, *193*, 673.